Int J Pharma Res Health Sci. 2018; 6 (2): 2522-27
DOI:10.21276/ijprhs.2018. 2018. 02.32
Jithendra and Krishnamurthy
CODEN (USA)-IJPRUR, e-ISSN: 2348-6465

PHS Scientific House
PHARMAHEALTHSCIENCES

International Journal of Pharma Research and Health Sciences

Available online at www.pharmahealthsciences.net

Original Article

Synthesis, Characterization and Antimicrobial Screening of Co(II) and Fe(III) Centered Magnetically Separable Transition Metal Nanocomposite

Jithendra Kumara K S[1], Krishnamurthy G [1, *]
Department of Chemistry, Sahyadri Science College, Shimoga, Karnataka-577203, India

ARTICLE INFO

Received: 12 Apr 2018
Accepted: 22 Apr 2018

ABSTRACT

The Co(II) and Fe(III) centres magnetically separable two new mesoporous nanoparticle were synthesised via chemical synthesis method. The transmission electron microscopic studies (TEM) show that, the particles are spherical shape with mean size of 20 nm. The X-ray diffraction spectrums of the synthesized nanoparticles were suggested that the nanoparticle size is veering from 25 to 30 nm the EDX spectrum reveals that SiO_2 is coating on the surface of the cobalt ferrate nanoparticle ($CoFe_2O_4$). The SiO_2 coating is efficiently preventing the aggregated collision of nanoparticles. The nanoparticle was simply separated by applying an external magnet to the reaction vessel and was re-dispersed into the next antimicrobial screening they showed exceptional stability against leaching and sintering.

Key words: Cobalt ferrite nanoparticle, Magnetic nanoparticles, Ferromagnetism, chemical method, antimicrobial activity,

1. INTRODUCTION

Interest in nanotechnologies and nanoscale materials has grown recently and their applications have attracted the attention of both the research and industrial communities in the chemical, environmental and medicinal sectors. Similarly, their successful application in membrane separation water treatment and purification processes has been demonstrated. The inspiration for integrating nano-technology and pharmacology has been growing

Corresponding author *
Dr Krishnamurthy G
Department of Chemistry,
Sahyadri Science College,
Shimoga, Karnataka-577203, India
Email: gkmnaiksahyadri@gmail.com

exponentially, predominantly in the areas of drug delivery with the objective of directing the drug to the disease site with minimal side effects and reducing the dosage through more localized and competent targeting. This involves the magnetic drug targeting, whereby an external magnetic field gradient is applied at the target tissue to deliver the drug through active targeting using high-affinity ligand attachment, as well as therapeutic strategies. In addition to this, nanotechnology is creating a myriad biomedical application such as tissue regeneration, antimicrobial application, gene transfection, and imaging [1-6]. The nano-dentistry uses several nanomaterials and dental nano robots to diagnose and treatment. The scope of such strategies includes a wide variety of oral health-related issues such as treatment of dentin hypersensitivity, bio-film elimination, diagnosis and treatment of oral cancers, bone replacement materials, and so on. Currently, newer technologies are being tested in endodontics, mainly towards the overcoming of the microbial challenge [7-12].

Cobalt ferrite ($CoFe_2O_4$) nanoparticles have exhibited high permeability, good saturation magnetization and no preferred direction of magnetization. Along with this, they exhibited a high coercivity of more than 5 kOe [13, 14]. The magnetic nanoparticles can be successfully modified to increase their biocompatibility and antibacterial activity before implementation as a drug delivery application. For example, a thin silver film coating onto Fe_3O_4 nanoparticles can improve antibacterial activity, as well as benefiting the paramagnetic properties of the nanostructures so that they can be recovered and recycled from the site of action by means of an external magnetic field [15]. In addition to this, oleic acid was used as a surface coating for Fe_3O_4 nanoparticles, followed by an adsorption coating with different antibiotics (cephalosporins) [16]. The coated ferrite nanoparticles showed good antimicrobial activity. Sanpo *et al*. execute zinc and copper substituted cobalt ferrite nanoparticles significantly improved antibacterial activity against *E. coli* and *S. aureus* [17].

Gopinath et al. demonstrated that eco-friendly approach for the synthesis of ruthenium nanoparticles (Ru NPs) using aqueous leaf extract, the synthesized nanoparticle exhibited good antibacterial performance against gram-positive and gram-negative bacterial strains [18]. Kannan, et. al. reported that [19] indicate leaf is capable of producing RuO_2 nanoparticles which exhibits good antibacterial activity against the microorganisms such as *S. marcescens*, *P. aeruginosa*, *E. coli* and *S. aureus*.

2. EXPERIMENTAL

2.1 Materials and Instrumentation

All reagents and starting materials were obtained commercially from Sigma-Aldrich and Merck, which were used as received without any further purification unless otherwise noted. Freshly distilled solvents were employed for all synthetic purposes. Spectroscopic grade solvents were employed for spectral works. All other chemicals were of AR grade. X-ray powder diffraction (XRD) patterns were recorded using a Cu Kα radiation source on a D8 Advance Bruker powder diffractometer. The magnetic measurements were performed on a Physical Property Measurement System (PPMS) from Quantum Design Inc. San Diego, USA equipped with a Vibrating Sample Magnetometer (VSM), Scanning electron microscopy studies were conducted on an S4800 Scanning Electron Microscope (SEM).Transmission Electron Microscopy (TEM,JEOL JEM-2010F (FEG, 80-200 kV) were used for morphological and chemical characterization of $CoFe_2O_4$ and SiO_2-$CoFe_2O_4$ nanoparticles.

2.2 Synthesis of Magnetic Cobalt Ferrite ($Co@Fe_2O_4$) Nanoparticles

The synthesis of magnetic cobalt ferrite nanoparticles was carried out by modification of reported procedure [20]. In a typical experiment, 25 mL of 0.4 M iron chloride and 25 mL of 0.2 M of cobalt chloride solutions were mixed at room temperature. 12.5 mL of 1.5 M NaCl solution was added dropwise slowly to the initially prepared mixture and then 3.0 M NaOH solution was added dropwise slowly with constant stirring until a pH of 11−12 reached. Finally, the mixture stirred for additional 1 hour at 80 ^oC in an ultrasonic bath. At the end of 1 hour, the solution was allowed to cool to room temperature and then was formed precipitate was collected by using an external magnet. The prepared $CoFe_2O_4$ nanoparticles washed 3 times with ultrapure water, re-dispersed, and stored in de-ionized water for further applications.

2.3 Synthesis of Magnetic Silica-Coated Cobalt Ferrite ($SiO_2/Co@Fe_2O_4$) Nanoparticles

In this experiment, 25 mL of 0.4 M iron chloride and 25 mL of 0.2 M cobalt chloride solutions were mixed at room temperature. 12.5 mL of 1.5 M NaCl solution was added slowly dropwise to the initially prepared mixture followed by the addition of 3.0 M NaOH solution slowly dropwise with constant stirring until the pH of 11−12 reached. Then 1 mL of tetraethylorthosilicate (TEOS) and 0.5 mL of NH_4OH were added to the reaction mixture. Finally, the mixture was stirred for additional 1 hour at 80 ^oC in an ultrasonic bath. The solution was allowed to cool to room temperature and then the precipitate was collected by using an external magnet. The prepared $SiO_2/Co@Fe_2O_4$ nanoparticles was washed 3 times with ultrapure water, re-dispersed and stored in de-ionized water for further applications.

2.4 Antibacterial screening.

The antibacterial activity of the above nanoparticles was tested against Gram positive bacteria namely *Staphylococcus*, *aureus*, and Gram-negative bacteria namely *Escherichia coli* and *Salmonella typhi* by agar well diffusion method. Twenty-four old Muller-Hinton broth cultures of test bacteria were swabbed on sterile Muller-Hinton agar plates using sterile cotton swab followed by punching wells of 6 mm with the help of sterile corkborer. The standard

drug (Chloramphenicol, 100 µg/mL of sterile distilled water), three different concentrations (100, 50 and 25 µg mL^{-1} in 10% distilled water) and control (10% distilled water) were added to respectively labeled wells. These plates were allowed to stand for 30 min. and incubated at 37 °C for 24 h in upright position and the zone of inhibition was recorded [21]. During this period, the test solution diffused zones of inhibition were recorded using Vernier callipers.

2.5 Antifungal screening.

The antifungal activity of the of the above nanoparticles was evaluated against *Aspergillus niger* and *Penicillium chrysogenum* fungus, using the sabouroud dextrose agar diffusion method [21]. Wells were made with a sterile corkborer (6 mm diameter). The standard drug (Fluconazole, 100 µg/mL of sterile distilled water) and control (10% distilled water) were added to respectively labeled wells. To these wells, 140µL from each (100, 50 and 25 µg/mL in 10% distilled water) of the test stock solution compounds were added and the plates were allowed to cool for an hour to facilitate the diffusion. The plates were then incubated at 37 °C for 48 h. At the end of the incubation period, the diameter of the zone of inhibition around the wells was measured using Vernier scale

3. RESULTS AND DISCUSSION

3.1. Characterization of metal nanoparticles

The various cobalt based magnetically separable nanoparticles have been synthesized. The magnetic cobalt ferrite nanoparticles ($Co@Fe_2O_4$) and Silica-Coated Cobalt Ferrite Nanoparticles ($SiO_2/Co@Fe_2O_4$) were synthesized by following a slightly modified version of literature procedures [18] i.e., by co-precipitation technique, the newly synthesized nanoparticles are characterized by X-ray diffraction spectroscopy. The Figure 1a and 1b show the X-ray diffraction pattern of the synthesized $Co@Fe_2O_4$ and $SiO_2/Co@Fe_2O_4$ nanoparticles respectively. Bragg reflections in the 2θ range of 5−80° (18.4, 30.3, 35.8, 43.3, 53.8, 57.4 and 63.8° for (111), (220), (311), (400), (422), (511) and (440) respectively) are assigned to a bare $Co@Fe_2O_4$ nanoparticle, the suggested phase with a cubic spinel structure (figure 1) (PDF Card 22−1086). The silica-coated cobalt ferrite nanoparticles X-ray diffraction also showed a similar diffraction with same 2θ range, during the calculation of particle size by using Scherer equation which gives 0-5 nm variation; therefore, it concluded that the silica-coated cobalt ferrite nanoparticles have slightly smaller particle size when compared with bare cobalt ferrite nanoparticles. Both Figures clearly show that the magnetic nanoparticles have more amorphous nature and the smaller amount of crystalline nature.

In order for further characterization of samples, Energy-Dispersive Spectrometry (EDX, Fig 2a, 2b) has been carried out. The figures show that Co metal atom is associated with the iron atom. Thus $CoFe_2O_4$ nanoparticles retained their identity even after silica coating and revealed that the magnetic nanoparticles were composed of the minor amount of carbon and oxygen atoms only no other impurities associated with this synthesized nanoparticles.

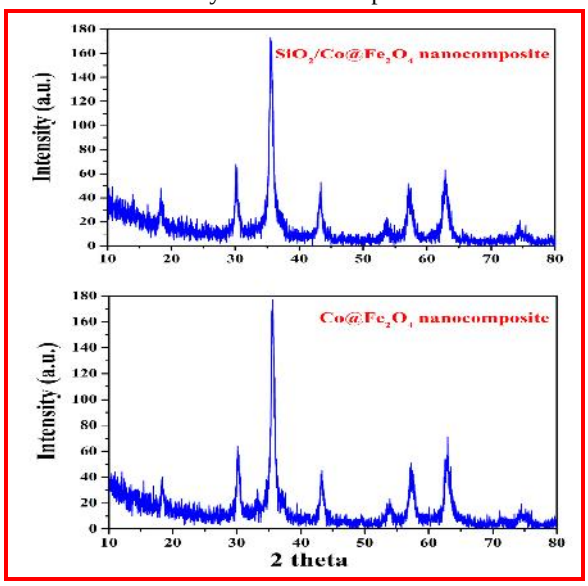

Fig 1: XRD patterns of $SiO_2/CoFe_2O_4$and $CoFe_2O_4$

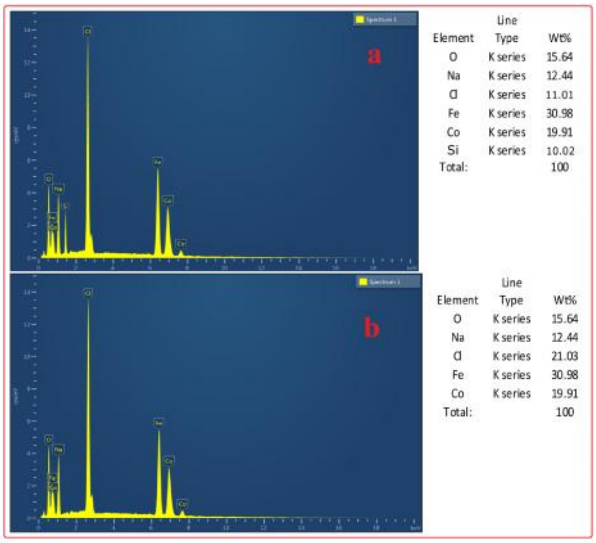

Fig 2: EDX spectrum of $SiO_2/CoFe_2O_4$ and $CoFe_2O_4$ nanoparticles with percentage of elements

The morphology and composition of cobalt ferrite ($Co@Fe_2O_4$) and silica-coated cobalt ferrite nanoparticles ($SiO_2/Co@Fe_2O_4$) were investigated by SEM analyses. The SEM images of Figure 7 show the aggregation of irregular spherical flakes, cobalt ferrite nanoparticles of about 15−35 nm size. The SEM images of silica-coated cobalt ferrite nanoparticles showed in fig 7c and 7d clearly shows the irregular spherical shape. Furthermore, silica coated nanoparticles were not as much aggregated like flakes when compared with bare cobalt ferrite nanoparticles. The particle sizes of $SiO_2/Co@Fe_2O_4$ nanoparticles are comparatively 0-5 nm smaller than bare $Co@Fe_2O_4$ hence it clearly indicates the TEOS quite stabilize the magnetic nanoparticles. The SEM images of $Co@Fe_2O_4$ nanoparticle represented in

Figure 3e-3f indicated that the spherical particles are in the form of flakes and the average particle size is about 25−35 nm, the SEM image of synthesized nanoparticles provides an only surface structure of the nanoparticles. It does not tell about inner core structure of the nanoparticles.

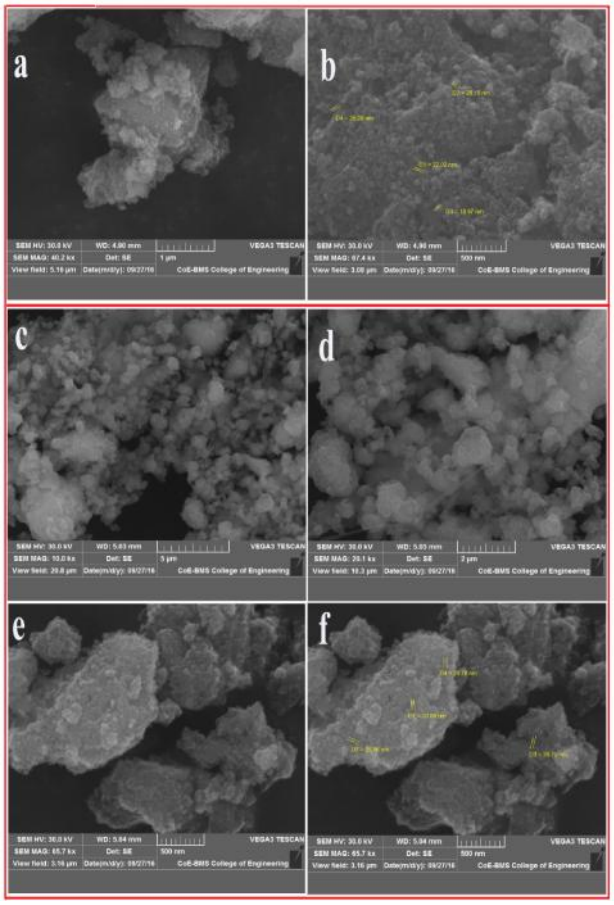

Fig 3: High-resolution SEM images of $SiO_2/CoFe_2O_4$ nanoparticles in different magnifications (a, b, c, d); high-resolution SEM image of $CoFe_2O_4$ nanoparticles (e, f)

The TEM pictures were collected for both bare $Co@Fe_2O_4$ and $SiO_2/Co@Fe_2O_4$ nanoparticle. The figures 4 (b, e) and 4 (a, d) are representative images of the bare $Co@Fe_2O_4$ and $SiO_2/Co@Fe_2O_4$ samples respectively, The analysis of TEM images is clearly shows that the estimation of thickness of the silica shell surrounded by the cobalt ferrite nanoparticles is quite difficult. In fact, while the measurement of the external diameter does not constitute a problem, the border between the core and the shell of the particles is not clearly measurable due to the poor "optical" contrast. For this reason, in Figure 4(d) and 8(e) we report only the external diameter of the $SiO_2/Co@Fe_2O_4$ nanoparticles. A comparison of the TEM micrographs evidence that bare cobalt ferrite nanoparticles existing as a larger size particles than $SiO_2/Co@Fe_2O_4$ nanoparticles.The cobalt ferrite nanoparticles show a relatively coherent coating with small black dots decorating the smooth silica surface owing to a loosely precipitating layer of thickness 15–25 nm. This result implies that the silica-coated cobalt ferrite nanoparticles consist of smaller subunits. Consequently, the obtained nanoparticles show the diameters in the range 5-10 nm. The synthesized magnetic nanoparticles show relatively narrow particle size distribution. Moreover, the lattice fringe is calculated from this image corresponds to (111) plane of cubic $Co@Fe_2O_4$ phase

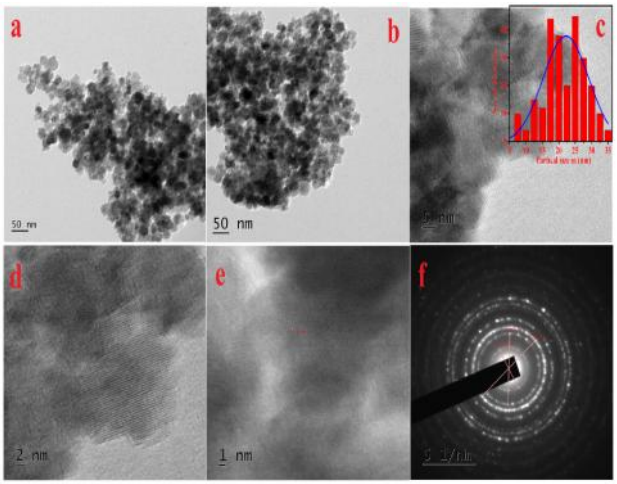

Fig 4: High-resolution TEM images of $CoFe_2O_4$ nanoparticles in different magnifications (a, d); high-resolution TEM image of $SiO_2/CoFe_2O_4$nanoparticles (b, e) particle size distribution bar graph (c) seed pattern of the $SiO_2/CoFe_2O_4$nanoparticles (f)

3.2 Antimicrobial activity assay

The result of the antibacterial and antifungal activity is tabulated in table 1 and result of the minimum inhibition concentration (MIC) is tabulated in table 2. The antimicrobial activity was compared with *Chloramphenicol*, *Fluconazole*, standard to ascertain its true potential. The above collective results showed that the silica coated cobalt ferrite nanocomposite, $SiO_2/Co@Fe_2O_4$ nanocomposite (1a) and $Co@Fe_2O_4$ nanocomposite (2a). Exhibited good antimicrobial action against all microbes' isolates tested, with the size of the zone of inhibition greater than 1 mm.

Table 1: Results of the antimicrobial activity zone of inhibition in mm

Compounds (µg/mL)	Growth Inhibition against Bacteria in mm			Growth Inhibition against Fungi in mm	
	S.aureus	***E.coil***	***S.typhi***	***A.niger***	***P.crysogenum***
1c 100	4.0 ± 0.1	7 ± 0.0	6.0 ± 0.0	4.0 ± 0.0	7.0 ± 0.0
1c 500	4.1 ± 0.1	8 ± 0.0	9.0 ± 0.0	6.3 ± 0.05	7.5 ± 0.1
1c 700	5.0 ± 0.1	10 ± 0.0	10.5 ± 0.05	9.1 ± 0.1	8.3 ± 0.05
2a 100	4.0 ± 0.0	10.0 ± 0.05	7.1 ± 0.1	1.0 ± 0.0	8 ± 0.0
2a 500	3.9 ± 0.1	11.5 ± 0.05	7.3 ± 0.05	3.9 ± 0.1	9.0 ± 0.0
2a 700	4.1 ± 0.1	13.0 ± 0.0	8.9 ± 0.1	4.0 ± 0.05	10 ± 0.05
Std 1* 100	4.9 ± 0.05	3.9 ± 0.05	3.9 ± 0.05	6.0 ± 0.0	7.0 ± 0.0
Std 1* 500	7.0 ± 0.0	7.0 ± 0.0	6.9 ± 0.05	9.0 ± 0.0	8.0 ± 0.0
Std 1* 700	8.0 ± 0.0	8.0 ± 0.0	8.0 ± 0.05	10.0 ± 0.0	9.0 ± 0.0
Std 2* 100				7 ± 0.0	7 ± 0.0
Std 2* 500				8 ± 0.0	8 ± 0.0
Std 2* 700				9 ± 0.0	9 ± 0.0

Less than 8mm - inactive; 10–12mm - moderately active; above 12mm - highly active [#]*Chloramphenicol*, [*]*Fluconazole*, (sample size n-3)

Silica coated cobalt ferrite nanocomposite, SiO_2/Co@Fe_2O_4 nanocomposite (1a), Co@Fe_2O_4 nanocomposite (2a).

Table 2: Results of the antimicrobial activity - Minimum inhibition concentration (MIC)

Compound Conc. (30 µg mL^{-1})	Growth inhibition against bacteria (in mm)			Growth inhibition against fungi (in mm)	
	S.aureus	***E. coil***	***S.typlei***	***A.Niger***	***P.Crysogenum***
1c	4 ± 0.1	10 ± 0.2	8 ± 0.1	7.5 ± 0.0	5 ± 0.1
2a	4.3 ± 0.2	10.5 ± 0.2	3 ± 0.0	1 ± 0.1	7 ± 0.0

Less than 8mm - inactive; 10–12mm - moderately active; above 12mm - highly active, (n-3)

Silica coated cobalt ferrite nanocomposite, SiO_2/Co@Fe_2O_4 nanocomposite (1a), Co@Fe_2O_4 nanocomposite (2a).

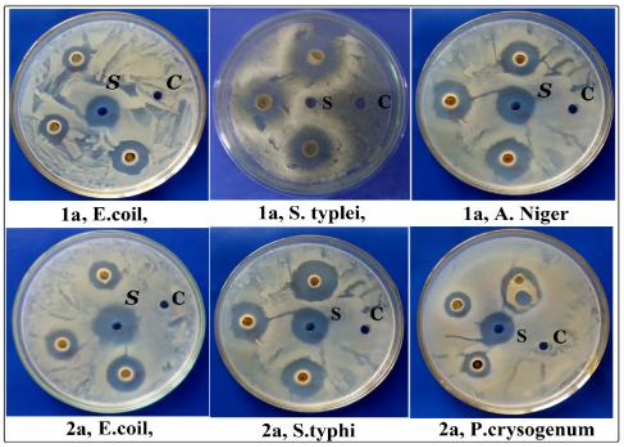

Fig 5: Inhibition of pathogenic bacteria and fungi in a dual culture and well diffusion method

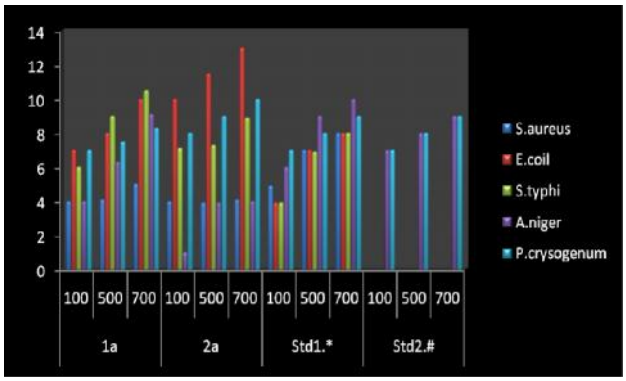

Fig 6: Bar graph representation of the antimicrobial activity

In the above nanocomposite, more precisely sample SiO_2/Co@Fe_2O_4, 1c and Co@Fe_2O_4, 2a exhibited the good antibacterial activity against *E. coli* bacteria with the zone of inhibition reaching a diameter of upto 10 mm and 9.6 mm respectively. In addition to this the sample1a and 2a exhibited moderate antibacterial activity against *S. aureus, A. Niger S. typlei*and *P. Crysogenum* bacterial species with a zone of inhibition diameter ranging from 3.5 mm to 8 mm. both the nanoparticles showed good activity *E. coli* bacteria is probably due to metal ion resistance mechanisms, such as active efflux and remaining samples showed moderately good activity.

The exact mechanism of metal nanoparticles on antibacterial activity has not yet been understood clearly.The possible potential mode of action is metal ions released from metallic nanoclusters can interact with thiol groups on essential bacterial enzymes, resulting in their inactivation and leading to cell death. The nanoparticles were first attach to the bacterial membrane by electrostatic interaction between the negatively charged bacterial cell and the positively charged nanoparticles is crucial for the activity of the nanoparticles as bactericidal material and this disrupts the integrity of the bacterial membrane and subsequently cell death takes place due to this structural change. The cobalt ferrite nanoparticles interference with the bacterial cell membrane and their binding with mesosome will thereby reduce the mesosomal function and increase the reactive oxygen species generation, which leads to cell death.Another mode of action, is membrane function, in which electrostatic interaction of the metal nanoparticles and the surface of the bacteria. This results in the aggregation of nanoclusters on the cell surface and change in cell morphology leading to growth inhibition.

4. CONCLUSION

In summary, the study of synthesis and characterization of bare Co@Fe_2O_4 nanoparticle and SiO_2/Co@Fe_2O_4 nanoparticle, these synthesized nanoparticles were screened for their antimicrobial activity which has been led to the following conclusions and insights. Both the nanoparticles can be easily and reproducibly prepared by co-precipitation method; the SiO_2/Co@Fe_2O_4 nanoparticles are showed potential antimicrobial activity with *E. coli* bacteria with metal ion resistance mechanisms. Further extension this type of nanoparticle synthesis and screening of their antimicrobial activity is underway in our laboratory.

5. ACKNOWLEDGEMENTS

The authors would like to thank Department of Chemistry, Sahyadri Science College, Shimoga, for providing experimental facilities, and we extended our thanks to Department of Industrial Chemistry, Kuvempu University, Shimoga, The authors acknowledge there is no grant and funding is resaved for this research work.

6. REFERENCES

1. Cohen ML. Nanotubes, Nanoscience, and Nanotechnology. Mater Sci Eng C. 2001; 15, 1-2.
2. Thomas J. Peppas N. Sato M. Webster T. Nanotechnology and biomaterials. In: Gogotsi Y, edt. Nanomaterials handbook, CRC Taylor and Francis,(2006).
3. Jithendra kumara KS, Krishnamurthy G, Kumara swamy BE, Shashi kumar ND, Satish naika, Krishna BS, Nagaraj naik, Terephthalic acid derived ligand-stabilized palladium nanocomposite catalyst for Heck coupling reaction: without surface-modified

heterogeneous catalyst, Appl. Organometal. Chem. 31 (2017) 3549
4. Venugopal J, Prabhakaran MP, Low S, Choon AT, Zhang YZ, Deepika G, Ramakrishna S, Nanotechnology for nanomedicine and delivery of drugs. Curr Pharm Des. 2008; 14, 2184-2200.
5. Jithendra Kumara KS, Krishnamurthy G, Swamy BEK, N. Kumar S, Kumar M. Sustainable Catalytic performance study of nano-cobalt: a catalyst for complement to the Heck coupling reaction. J Porous Mater. 2017; 24, 1095-1103
6. Cushing BL, Kolesnichenko VL, Connor CJO. Recent Advances in the Liquid-Phase Syntheses of Inorganic Nanoparticles. Chem Rev. 2004; 104, 3893.
7. Costerton JW, Lewandowski Z, De Beer D, Caldwell D, Korber D, James G. Biofilms, the customized microniche. J Bacteriol. 1994; 176, 2137-2142.
8. Del Pozo JL, Patel R. The challenge of treating biofilm-associated bacterial infections. Clin. Pharmacol. Ther. 2007; 82, 204-209.
9. Khan, ZUH, Khan A, Chen YM, Shah NS, Muhammad N, Khan AU, Tahir K, Khan FU, Murtaza B, Hassan SU, Qaisrani SA, Wan P. Biomedical applications of green synthesized Nobel metal nanoparticles. J. Photochem. Photobiol. B. Biology. 2017; 173, 150-164.
10. Dizaj SM, Lotfipour F, Jalali MB, Zarrintan MH, Adibkia K. Antimicrobial activity of the metals and metal oxide nanoparticles. Mater Sci Eng C Mater Biol Appl. 2014; 44, 278-284.
11. Singh TH, Dharambir K, Kaur BS, Pardeep K, Gaurav K, Singh SS. Molecular aspects of metal oxide nanoparticle (MO-NPs) mediated pharmacological effects. Life Sci. 2015; 143, 71-79.
12. Sportelli MC, Picca RA, Cioffi N. Recent advances in the synthesis and characterization of nano-antimicrobials. () Trends Anal. Chem. 2016; 84, 131-138. doi: 10.1016/j.trac.2016.05.002.
13. Meng X, Li H, Chen J, Mei L, Wang K, Li X. Mössbauer study of cobalt ferrite nanocrystals substituted with rare-earth Y^{3+} ions. J Magn Magn Mater. 2009; 321, 1155-1158.
14. Phua LX, Xu F, Ma YG, Ong CK. Structure and magnetic characterizations of cobalt ferrite films prepared by spray pyrolysis. Thin Solid Film. 2009; 517, 5858-5861.
15. Sun S, Zeng H, Robinson DB, Raoux S, Rice PM, Wang SX. Monodisperse MFe_2O_4 (M = Fe, Co, Mn) Nanoparticles. J Am Ceram Soc. 2004; 126, 273-279.
16. Buteica AS, Mihaiescu DE. Grumezescu AM, Vasile BS, Popescu A, Mihaiescu OM. The anti-bacterial activity of magnetic nanofluid: Fe_3O_4 /oleic acid/cephalosporins core/shell/adsorptionshell proved on s. aureus and e. coli and possible applications as drug delivery systems. Dig J Nanometer Bios. 2010; 5, 927-932.
17. Sanpo N, Berndt CC, Wen C, Wang J. Transition metal-substituted cobalt ferrite nanoparticles for biomedical applications. Acta Biomaterialia. 2013; 9, 5830-5837.
18. Gopinath K, Karthika V, Gowri S, Senthilkumar V, Kumaresan S, Arumugam A. Antibacterial activity of ruthenium nanoparticles synthesized using Gloriosa superba L. leaf extract. J Nanostruct Chem. 2014; 4, 83, 1-6
19. Kannan SK, Sundrarajan M. Green synthesis of ruthenium oxide nanoparticles: Characterization and its antibacterial activity. Advanced Powder Technology, 2015; 26, 6, 1505-1511.
20. Kaya M, Zahmakiran M, zkar SO, Volkan MR. Copper(0) Nanoparticles Supported on Silica-Coated Cobalt Ferrite Magnetic Particles: Cost Effective Catalyst in the Hydrolysis of Ammonia-Borane with an Exceptional Reusability Performance, ACS Appl. Mater. Interfaces. 2012; 4 3866-3873.
21. Shashikumar ND, Krishnamurthy G, Bhojyanaik HS, Lokesh M, Jithendrakumara KS. Synthesis of new biphenyl-substituted quinoline derivatives, preliminary screening and docking studies. J. Chem. Sci. 2014; 126, 205-212.

Conflict of Interest: None

Source of Funding: Nil